The Journal of PHARMACOLOGY And Experimental Therapeutics

Plumbagin (5-Hydroxy-2-methyl-1,4-naphthoquinone) Induces Apoptosis and Cell Cycle Arrest in A549 Cells through p53 Accumulation via c-Jun NH₂-Terminal Kinase-Mediated Phosphorylation at Serine 15 in Vitro and in Vivo

Ya-Ling Hsu,[1] Chien-Yu Cho,[1] Po-Lin Kuo, Yu-Ting Huang, and Chun-Ching Lin

Department of Biotechnology, Chia-Nan University of Pharmacy and Science, Tainan, Taiwan (Y.-L.H., P.-L.K., Y.-T.H.); and Graduate Institute of Natural Products, College of Pharmacy, Kaohsiung Medical University, Kaohsiung, Taiwan (C.-Y.C., C.-C.L.)

ABSTRACT

This study first investigates the anticancer effect of plumbagin (5-hydroxy-2-methyl-1,4-naphthoquinone) in human nonsmall cell lung cancer cells, A549. Plumbagin has exhibited effective cell growth inhibition by inducing cancer cells to undergo G_2/M phase arrest and apoptosis. Blockade of cell cycle was associated with increased levels of p21 and reduced amounts of cyclinB1, Cdc2, and Cdc25C. Plumbagin treatment also enhanced the levels of inactivated phosphorylated Cdc2 and Cdc25C. Blockade of p53 activity by dominant-negative p53 transfection partially decreased plumbagin-induced apoptosis and G_2/M arrest, suggesting it might be operated by p53-dependent and independent pathway. Plumbagin treatment triggered the mitochondrial apoptotic pathway indicated by a change in Bax/Bcl-2 ratios, resulting in mitochondrial membrane potential loss, cytochrome *c* release, and caspase-9 activation. We also found that c-Jun NH₂-terminal kinase (JNK) is a critical mediator in plumbagin-induced cell growth inhibition. Activation of JNK by plumbagin phosphorylated p53 at serine 15, resulting in increased stability of p53 by decreasing p53 and MDM2 interaction. SP600125 (anthra [1,9-*cd*]pyrazol-6(2*H*)-one-1,9-pyrazoloanthrone), a specific inhibitor of JNK, significantly decreased apoptosis by inhibiting the phosphorylation of p53 (serine 15) and subsequently increased the interaction of p53 and MDM2. SP600125 also inhibited the phosphorylation of Bcl-2 (Ser70) induced by plumbagin. Further investigation revealed that plumbagin's inhibition of cell growth effect was also evident in a nude mice model. Taken together, these results suggest a critical role for JNK and p53 in plumbagin-induced G_2/M arrest and apoptosis of human nonsmall cell lung cancer cells.

Lung cancer is one of the leading causes of death in the world, and nonsmall cell lung carcinoma accounts for approximately 75 to 85% of all lung cancers (Raez and Lilenbaum, 2004). Nonsmall cell lung cancers commonly develop resistance to radiation and chemotherapy and often present at stages too late for surgical intervention. Since current treatment modalities are inadequate, novel therapies are needed to reduce the effects of the increasing incidence in pulmonary neoplasm (Raez and Lilenbaum, 2004; Kelly, 2005).

The tumor suppressor protein p53 is targeted by a wide variety of intracellular and extracellular stimuli, such as withdrawal of growth factors, hypoxia, irradiation, chemicals, and defects in nucleotide synthesis (Harris and Levine, 2005). The activation of p53 leads, primarily through its transcriptional function, to either apoptosis, eliminating those cells harboring severely damaged DNA, or growth arrest, allowing damaged DNA to be repaired and thereby suppressing tumor formation (Harris Robles et al., 2002; Levine, 2005). Stability and activity of p53 are believed to be regulated in part by posttranslational modifications, such as phosphorylation and acetylation. Phosphorylation on NH₂-terminal residues, especially Ser15, Thr18, Ser20, and Ser37, is believed to affect interaction with the negative regulator

ABBREVIATIONS: JNK, c-Jun NH₂-terminal kinase; plumbagin, 5-hydroxy-2-methyl-1,4-naphthoquinone; DMSO, dimethyl sulfoxide; PI, propidium iodide; SP600125, anthra [1,9-*cd*]pyrazol-6(2*H*)-one-1,9-pyrazoloanthrone; phospho-JNK, phosphorylated c-Jun NH₂-terminal kinase; XTT, sodium 3′-[1-(phenylamino-carbonyl)-3,4-tetrazolium]-bis(4-methoxy-6-nitro)benzene-sulfonic acid hydrate; TUNEL, terminal deoxynucleotidyl transferase dUTP nick-end labeling; CHAPS, 3-[(3-cholamidopropyl)dimethylammonio]-1-propanesulfonic acid; JC-1, 5,5′,6,6′-tetrachloro-1,1′,3,3′-tetraethylbenzimidazolylcarbocyanine iodide; G418, geneticin; PARP, poly(ADP-ribose) polymerase.

MDM2 and hence contribute to the stabilization of p53. Phosphorylation on COOH-terminal Ser315 and Ser392 in particular is believed to enhance the specific DNA binding of p53 in vitro (Xu, 2003; Bode and Dong, 2004).

c-Jun NH$_2$-terminal kinase (JNK), a member of the mitogen-activated protein kinase family protein kinases, is an important member of the signal transduction pathway that transduces extracellular signals in intracellular responses and has been implicated in a wide array of physiological processes, including cell growth, differentiation, and apoptosis (Liu and Lin, 2005). JNK can induce apoptosis in response to a variety of stresses. The proposed mechanisms of this effect are the change of gene expression as well as eliciting its phosphorylation activity to several specific substrates (Liu and Lin, 2005). Activated JNK phosphorylates and stabilizes p53 by abrogating MDM2 association (Fuchs et al., 1998; Buschmann et al., 2000). Recent studies have shown that JNK activation is required for stress-induced release of mitochondrial cytochrome *c* and for apoptosis mediated by the mitochondrial caspase-9 pathway (Chen et al., 2003; Gao et al., 2005; Zu et al., 2005). Several proapoptotic factors have indicated that phosphorylation by JNK enhances proapoptotic activity (Liu and Lin, 2005; Yoshida et al., 2005). In addition, phosphorylation of prosurvival Bcl-2 by JNK disrupts the binding motif of Bcl-2 and makes it unable to antagonize Bax (Zu et al., 2005).

Plumbagin, a quinonoid constituent isolated from the root of *Plumbago zeylanica* L., has been shown to exert anticarcinogenic, antiatherosclerotic, and antimicrobial effects (Mossa et al., 2004; Srinivas et al., 2004; Ding et al., 2005; Hsieh et al., 2005). It exhibits an inhibitory effect on carcinogenesis in the intestines, causes cytogenetic and cell cycle changes in mouse Ehrlich ascites carcinoma, and possesses antiproliferation activity in human cervical cancer cells (Singh and Udupa, 1997; Sugie et al., 1998; Srinivas et al., 2004). In this study, we determined the cell growth inhibition activity of plumbagin by using in vitro and in vivo experimental models and examined its effect on cell cycle distribution and apoptosis in human nonsmall cell lung cancer cell A549. Furthermore, to establish plumbagin's anticancer mechanism, we assayed the levels of cell cycle control- and apoptosis-related molecules, which are strongly associated with the programmed cell death signal transduction pathway and affect the chemosensitivity of tumor cells to anticancer agents.

Materials and Methods

Reagents. Fetal calf serum and RPMI 1640 were obtained from GIBCO BRL (Gaithersburg, MD). Plumbagin, dimethyl sulfoxide (DMSO), RNase, and propidium iodide (PI) were purchased from Sigma Chemical Co. (St. Louis, MO). JNK inhibitor SP600125 and Bcl-Xs antibody were purchased from Calbiochem (Cambridge, MA). The antibodies to β-actin, cyclinB1, Cdc2, Cdc25C, p21, Bax, Bak, Bcl-2, phospho-Bcl-2, and Bcl-X$_L$ were obtained from Santa Cruz Biotechnology (Santa Cruz, CA). The antibodies to p53, phospho-p53, MDM2, JNK, phospho-JNK, phospho-Cdc2, phospho-Cdc25C, and cytochrome *c* were obtained from Cell Signaling Technology (Beverly, MA). The pCMV and pCMV-p53mt135 plasmids were supplied by CLONTECH (Palo Alto, CA). Lipofectamine 2000 reagent was obtained from Life Technologies, Inc. (Rockville, MD). COS cells plus UV irradiation cell extract was obtained from Laprice (Brussels, Belgium). MCF-7 cells plus UV irradiation cell extract was obtained from Active Motif (Carlsbad, CA).

Cell Culture. A549 (American Type Culture Collection CCL185; American Type Culture Collection, Manassas, VA) was maintained in RPMI 1640 supplemented with 10% FBS, 10 U/ml penicillin, 10 μg/ml streptomycin, and 0.25 μg/ml amphotericin B. IMR-90 (American Type Culture Collection CCL-186) fibroblast cells were cultured in minimum essential medium (Eagle) with Earle's balanced salt solution, 2 mM L-glutamine, 1.5 mg/ml sodium bicarbonate, 0.1 mM nonessential amino acids, 1.0 mM sodium pyruvate, 10 U/ml penicillin, 10 μg/ml streptomycin, 0.25 μg/ml amphotericin B, and 10% fetal calf serum. Both cell lines were cultured in monolayer culture at 37°C and 5% CO$_2$.

Cell Proliferation and Clonogenic Assay. Inhibition of cell proliferation by plumbagin was measured by sodium 3′-[1-(phenylamino-carbonyl)-3,4-tetrazolium]-bis(4-methoxy-6-nitro)benzenesulfonic acid hydrate (XTT) assay. In brief, cells were plated in 96-well culture plates (1×10^4 cells/well). After 24-h incubation, the cells were treated with plumbagin (0, 2.5, 5, 10, and 20 μM) for 6, 12, 24, and 48 h. An amount of 50 μl of XTT test solution, which was prepared by mixing 5 ml of XTT-labeling reagent with 100 μl of electron coupling reagent, was then added to each well. After 4 h of incubation, the absorbance was measured on an enzyme-linked immunosorbent assay reader (Multiskan EX; Thermo Electron, Waltham, MA) at a test wavelength of 492 nm and a reference wavelength of 690 nm.

To determine the long-term effects, cells were treated with plumbagin at various concentrations for 1 h. After being rinsed with fresh medium, cells were allowed to grow for 14 days to form colonies that were then stained with crystal violet (0.4 g/l; Sigma). Clonogenic assay was used to elucidate the possible differences in long-term effects of plumbagin in A549 and IMR-90 cells.

Cell Cycle Analysis. To determine cell cycle distribution analysis, 5×10^5 cells were plated in 60-mm dishes and treated with plumbagin (0, 10, and 20 μM) for 6 h. After treatment, the cells were collected by trypsinization, fixed in 70% ethanol, washed in phosphate-buffered saline, resuspended in 1 ml of phosphate-buffered saline containing 1 mg/ml RNase and 50 μg/ml PI, incubated in the dark for 30 min at room temperature, and analyzed by EPICS flow cytometer. The data were analyzed using Multicycle software (Phoenix Flow Systems, San Diego, CA).

Apoptosis Assay. Cells (1×10^6) were treated with vehicle alone (0.1% DMSO) and various concentrations of plumbagin for indicated times and then collected by centrifugation. Pellets were lysed by DNA lysis buffer (10 mM Tris, pH 7.5, 400 mM EDTA, and 1% Triton X-100) and then centrifuged. The supernatant obtained was incubated overnight with proteinase K (0.1 mg/ml), then with RNase (0.2 mg/ml) for 2 h at 37°C. After extraction with phenol/chloroform (1:1), the DNA was separated in 2% agarose gel and visualized by UV after staining with ethidium bromide.

Quantitative assessment of apoptotic cells was assessed by the terminal deoxynucleotidyl transferase dUTP nick-end labeling (TUNEL) method, which examines DNA strand breaks during apoptosis by using BD ApoAlert DNA Fragmentation Assay Kit. In brief, cells were incubated with 0, 10, and 20 μM plumbagin for the indicated times. The cells were trypsinized, fixed with 4% paraformaldehyde, and permeabilized with 0.1% Triton X-100 in 0.1% sodium citrate. After being washed, the cells were incubated with the reaction mixture for 60 min at 37°C. The stained cells were then analyzed with an EPICS flow cytometer and a fluorescence microscope at 20× magnification.

Assay for Caspase-9 Activity. The assay is based on the ability of the active enzyme to cleave the chromophore from the enzyme substrate of caspase-9, LEHD-pNA (Ac-Leu-Glu-His-Asp-pNA). Cell lysates were incubated with peptide substrate in assay buffer (100 mM NaCl, 50 mM HEPES, 10 mM dithiothreitol, 1 mM EDTA, 10% glycerol, and 0.1% CHAPS, pH 7.4) for 2 h at 37°C. The release of *p*-nitroaniline was monitored at 405 nm. Results are represented as the percentage of change in activity compared with the untreated control.

Mitochondrial Membrane Potential Assay. We used mitochondrial-specific cationic dye JC-1 (Invitrogen, Carlsbad, CA), which undergoes potential-dependent accumulation in the mitochondria. It is a monomer when the membrane potential ($\Delta\Psi$) is lower than 120 mV and emits a green light (540 nm) following excitation by blue light (490 nm). At higher membrane potentials, JC-1 monomers convert to J-aggregates that emit a red light (590 nm) following excitation by green light (540 nm). Cells were seeded in a 96-well plate. Following treatment with various concentrations of plumbagin for 8 and 12 h, cells were stained with 25 μM JC-1 for 30 min at 37°C. Fluorescence was monitored with the fluorescence plate reader at wavelengths of 490 nm (excitation)/540 nm (emission) and 540 nm (excitation)/590 nm (emission) pairs. Changes in the ratio between the measurement at test wavelengths of 590 nm (red) and 540 nm (green) fluorescence intensities are indicative of changes in the mitochondrial membrane potential (Martin and Forkert, 2004).

Immunoprecipitation/Immunoblot and JNK Activity Assays. Cells were treated with 20 μM plumbagin in the absence or presence of JNK inhibitors for specified intervals of time. Mitochondrial and cytoplasmic fractions were separated using Cytochrome c Releasing Apoptosis Assay Kit (BioVision, Mountain View, CA). For immunoblotting, the cells were lysed on ice for 40 min in a solution containing 50 mM Tris, 1% Triton X-100, 0.1% SDS, 150 mM NaCl, 2 mM Na_3VO_4, 2 mM EGTA, 12 mM β-glycerolphosphate, 10 mM NaF, 16 μg/ml benzamidine hydrochloride, 10 μg/ml phenanthroline, 10 μg/ml aprotinin, 10 μg/ml leupeptin, 10 μg/ml pepstatin, and 1 mM phenylmethylsulfonyl fluoride. The cell lysate was centrifuged at 14,000g for 15 min, and the supernatant fraction was collected for immunoblotting. Equivalent amounts of protein were resolved by SDS-polyacrylamide gel electrophoresis (10–12%) and transferred to polyvinylidene difluoride membranes. After blocking for 1 h in 5% nonfat dry milk in Tris-buffered saline, the membrane was incubated with the desired primary antibody for 1 to 16 h. The membrane was then treated with appropriate peroxidase-conjugated secondary antibody, and the immunoreactive proteins were detected using an enhanced chemiluminescence kit (GE Healthcare, Little Chalfont, Buckinghamshire, UK) according to the manufacturer's instructions.

For association of p53 and MDM2, cell lysates (300 μg) were incubated with 10 μl of anti-MDM2 for 1 h at 4°C. Immunocomplexes were resolved by 7.5% SDS-polyacrylamide gel electrophoresis. Association of MDM2 with p53 was detected by incubating the blots with anti-MDM2 and anti-p53 antibodies as described above. The JNK mitogen-activated protein kinase activities were determined using kits from Cell Signaling Technology according to the manufacturer's instructions.

Stable Transfection. Transfection of A549 cells was carried out using Lipofectamine 2000 reagent (Life Technologies). A549 cells were exposed to the mixture of Lipofectamine 2000 reagent and pCMV-p53mt135 plasmid or empty vector for 6 h. After transfection, cells resistant to neomycin were selected by incubating with medium containing 1 mg/ml G418 (Life Technologies), individual A549 clones were isolated and tested for constitutive p53 expression. The p53-positive A549 cells were selected and maintained in the presence of G418 (400 μg/ml), as were p53-negative control cells (Xu et al., 2003).

In Vivo Tumor Xenograft Study. Male nude mice [6 weeks old; BALB/cA-nu (nu/nu)] were purchased from the National Science Council Animal Center (Taipei, Taiwan) and maintained in pathogen-free conditions. A549 cells were injected s.c. into the flanks of nude mice (5×10^6 cells in 200 μl). Tumors were allowed to develop for ~20 days until they reached ~75 mm³, when treatment was initiated. Thirty mice were randomly divided into two groups. The mice in the plumbagin-treated group were i.p. injected with plumbagin in 25% polyethylene glycol (2 mg/kg body weight) in a 0.2-ml volume. The control group was treated with an equal volume of vehicle. After transplantation, tumor size was measured using calipers, and tumor volume was estimated according to the formula: tumor volume (millimeters cubed) = $L \times W^2/2$, where L is the length, and W is the width.

Analysis of apoptotic cells in formalin-fixed specimens was by BD ApoAlert DNA Fragmentation Assay Kit as described above. The apoptotic cells were detected using a fluorescent microscope at 20× magnification.

Statistical Analysis. Data were expressed as means ± S.D. Statistical comparisons of the results were made using analysis of variance. Significant differences ($p < 0.05$) between the means of control and plumbagin-treated cells were analyzed by Dunnett's test.

Results

Plumbagin Inhibits Cell Proliferation and Clonogenic Survival in A549 Cells. To investigate the potential cell proliferative inhibition activity of plumbagin in lung cancer, we first examined the effect of plumbagin on cell proliferation and clonogenic survival in A549 cells. As shown in Fig. 1A, plumbagin inhibited cell proliferation in A549 cancer cell lines in a concentration- and time-dependent manner. Maximal proliferation inhibition was observed at 48 h with 20 μM plumbagin, which inhibited proliferation in 81.98% of A549 cells and had an IC_{50} value of 11.69 μM.

We performed in vitro clonogenic assays to determine the antitumor activities of plumbagin inhibition. The in vitro clonogenic assays correlate very well with in vivo assays of tumorigenicity in nude mice (Freedman and Shin, 1974; Shin et al., 1975). Figure 1, B and C, shows the effects of plumbagin on the relative clonogenicity of the control and the plumbagin-treated A549 cells. Clonogenicity of A549 cells was reduced in a dose-dependent manner after exposure to plumbagin.

To examine the selection of plumbagin-mediated cell proliferation inhibition, we also evaluated the effect of plumbagin in the normal lung cell line, IMR-90. The results showed that treatment of IMR-90 cells with plumbagin failed to affect the cell proliferation at any of the examined time points (Fig. 1D). In addition, plumbagin also failed to affect the colony formation in IMR-90 cells (Fig. 1, E and F). This result demonstrated that plumbagin possessed selectivity between normal and cancer cells.

Plumbagin Induces Cell Cycle Arrest and Apoptosis in A549 Cells. To examine the mechanism responsible for plumbagin-mediated cell proliferation inhibition, cell cycle distribution was evaluated using flow cytometric analysis. The results showed that treating cells with plumbagin caused a significant inhibition of cell cycle progression in A549 cells at 6 h (Fig. 2A), resulting in a clear increase of the percentage of cells in the G_2/M phase compared with the control.

We next assessed the effect of plumbagin on the induction of apoptosis in A549 cells by DNA fragmentation assay. The results showed that plumbagin treatment results in the formation of DNA fragments in A549 cells, as determined by agarose gel electrophoresis in a dose-dependent manner at 48 h and a time-dependent manner at a concentration of 20 μM (Fig. 2, B and C). A quantitative evaluation was also made using TUNEL to detect DNA strand breaks. Compared with vehicle-treated cells, 20 μM plumbagin induced 32.9 and 39% of apoptotic cells in A549 cells at 24 and 48 h, respectively (Fig. 2D). TUNEL-positive cells were also visible using a fluorescence microscope (Fig. 2E). Apoptosis was also evident upon examination of common molecular markers of apoptosis, including the cleavage of the caspase substrate PARP into the 89-kDa cleavage product and caspase-3 acti-
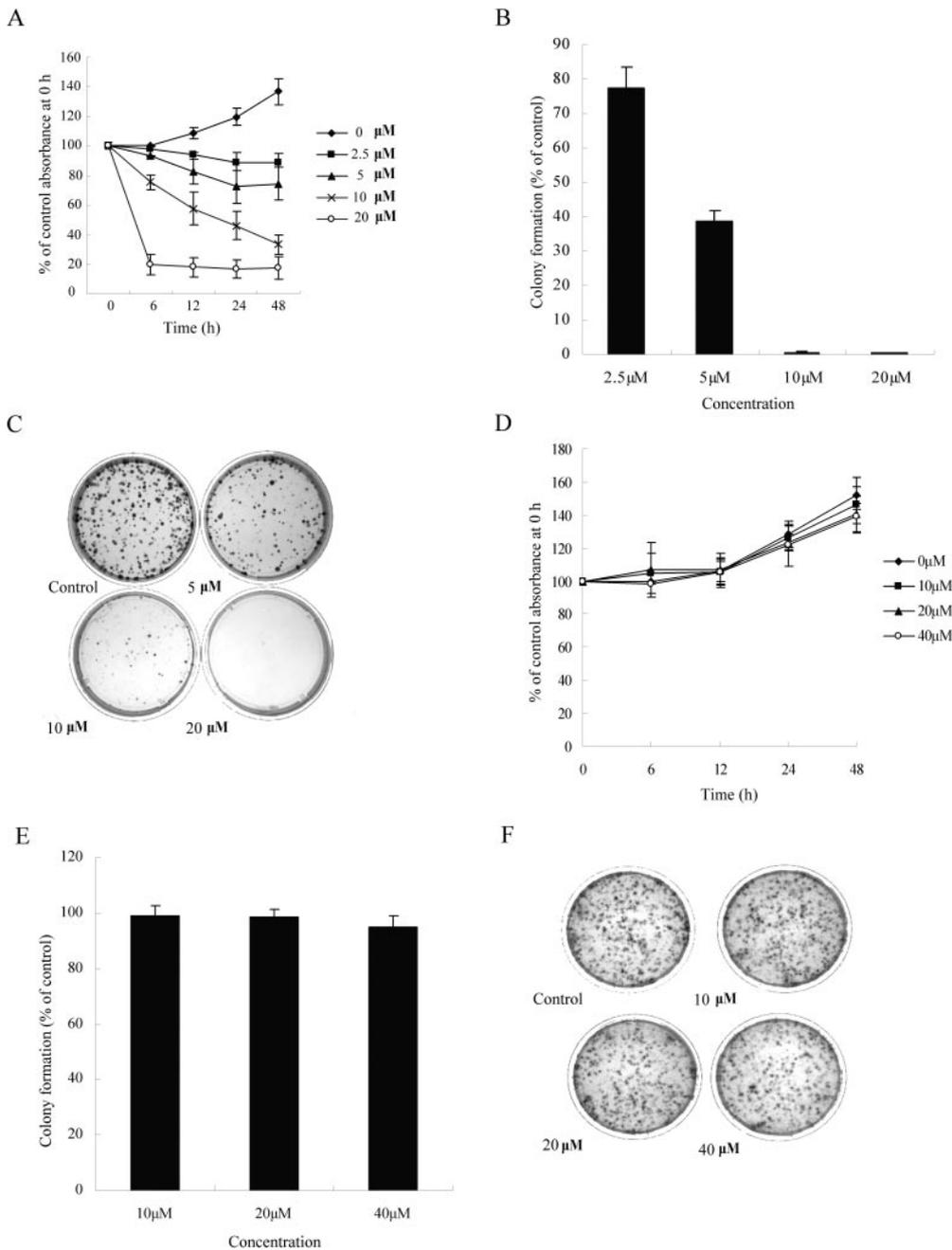
Fig. 1. The effects of plumbagin on cell proliferative inhibition and colony formation in A549 and IMR-90 cells. A, cell proliferative inhibition effect of plumbagin in A549. B, influence of A549 on the number of colony-forming cells as evaluated by clonogenic assay. C, representative dishes by colony-forming assay. D, cell proliferative inhibition effect of plumbagin in IMR-90. E, influence of IMR-90 on the number of colony-forming cells as evaluated by clonogenic assay. F, representative dishes by colony-forming assay. For A and D, cell growth inhibition activity of plumbagin was assessed by XTT. For colony-forming assay, the clonogenic assay was performed as described under *Materials and Methods*. Results of XTT are expressed as the percentage of cell proliferation of the control at 0 h. The data shown are the mean from three independent experiments. Each value is the mean ± S.D. of three determinations. ∗, significant difference between control and plumbagin-treated cells, as analyzed by Dunnett's test ($p < 0.05$).

vation. Plumbagin treatment induced both of these markers, which was consistent with the results of DNA fragmentation analysis (Fig. 2F).

To examine the selection of plumbagin-mediated G_2/M phase arrest and apoptosis, we also evaluated the effects of plumbagin in IMR-90. The results showed that treatment of IMR-90 cells with plumbagin failed to affect the distribution of cell cycle in IMR-90 cells after 6 h of treatment (Fig. 2G). In addition, plumbagin also failed to induce apoptosis in IMR-90 cells after 24 and 48 h of treatment (Fig. 2H). This result demonstrated that plumbagin possessed selectivity between normal and cancer cells.

Plumbagin Increases the Expression of p53 and Phosphorylated p53 (Ser15 and Ser392) and Regulates the Levels of Cell Cycle-Related Molecules in A549 Cells. Because our studies have shown that plumbagin treat-

ment of A549 cells results in G_2/M phase cell cycle arrest, we examined the effect of plumbagin on cell cycle-regulatory molecules, including p53, p21, cyclinB1, Cdc25C, and Cdc2. We first assessed the status of p53 in plumbagin-treated A549 cells. Exposure of cells to 20 μM plumbagin enhanced the phosphorylation of p53 on Ser15 and Ser392 (Fig. 3A) without any phosphorylation on serine residues 6, 9, 20, and 46. Plumbagin treatment was also associated with an increase in cells' levels of both p53 and its downstream target, p21 (Fig. 3A). In addition, the association of p53 and MDM2 decreased in a time-dependent manner in plumbagin-treated A549 cells, as detected by immunoprecipitation assay (Fig. 3B).

Next, we assessed the effects of plumbagin on cell cycle-related regulating factor. Plumbagin treatment of the cells resulted in a time-dependent decrease in the protein expres-
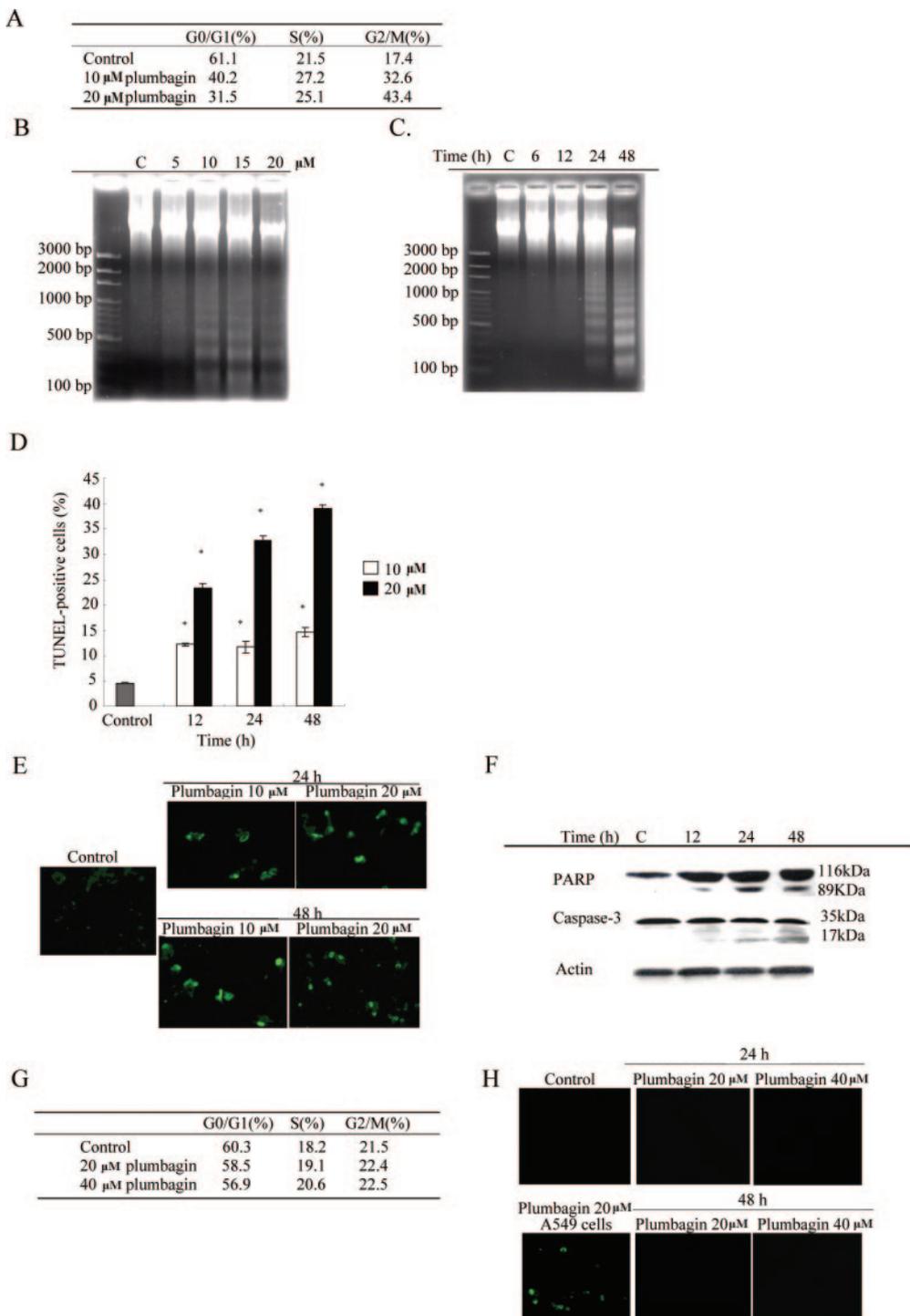
A

	G0/G1(%)	S(%)	G2/M(%)
Control	61.1	21.5	17.4
10 μM plumbagin	40.2	27.2	32.6
20 μM plumbagin	31.5	25.1	43.4

B

C.

D

E

F

G

	G0/G1(%)	S(%)	G2/M(%)
Control	60.3	18.2	21.5
20 μM plumbagin	58.5	19.1	22.4
40 μM plumbagin	56.9	20.6	22.5

H

Fig. 2. The effect of plumbagin on cell cycle arrest and apoptosis in A549 cells. A, distribution of cell cycles in plumbagin-treated cells. The DNA fragmentation of A549 induced by plumbagin as determined by electrophoresis assay at 48 h by various concentrations of plumbagin treatment (B) and the time course by 20 μM plumbagin treatment (C). Quantitative evaluations of TUNEL assay by flow cytometry (D) and fluorescence microscope (E). The cleavage of PARP and caspase-3 in A549 cells (F). The effect of plumbagin on cell cycle distribution (G) and apoptosis induction in IMR-90 cells (H). For A and G, cells were treated with vehicle and plumbagin for 6 h, and cell cycle distribution was assessed by flow cytometry. For B and C, cells were treated with various concentrations of plumbagin for the indicated times, and then DNA fragmentation was assessed by agarose gel electrophoresis. For D, E, and H, the TUNEL-positive cells were examined by flow cytometry and were visible through fluorescence microscope. For F, the cleavage of PARP and caspase-3 was determined by immunoblot assay. Each value is the mean ± S.D. of three determinations. *, significant difference between control and plumbagin-treated cells, as analyzed by Dunnett's test ($p < 0.05$).

sion of cyclinB1, Cdc2, and Cdc25C in A549 cells (Fig. 3C). In addition, exposure of cells to plumbagin for 3 h resulted in an increase in the levels of inactive phospho-Cdc2 (Tyr15) and phospho-Cdc25C (Ser216). Results from time-dependent studies have indicated that decreasing functional Cdc25C by increasing phosphorylation was followed by an increase in phospho-Cdc2 (Fig. 3C). We suggest that Cdc2 action was inhibited by a decrease in Cdc25C expression.

Plumbagin Induces the Execution of Apoptosis through Activation of the Mitochondrial Pathway. To investigate the mitochondrial apoptotic events involved in plumbagin-induced apoptosis, we first analyzed the changes

in the levels of proapoptotic proteins Bax, Bak, and Bcl-Xs, and antiapoptotic proteins Bcl-2 and Bcl-X$_L$. Western blot analysis showed that treatment of A549 cells with plumbagin increased Bax, Bak, and Bcl-Xs protein levels (Fig. 3A). In contrast, plumbagin decreased Bcl-2 and Bcl-X$_L$ levels, which led to an increase in the proapoptotic/antiapoptotic Bcl-2 ratio (Fig. 4A). In addition, plumbagin also increased phosphorylation of Bcl-2 (Ser70) in A549 cells.

Both mitochondrial depolarization and the loss of cytochrome c from the mitochondrial intermembrane space have been proposed as the early events during apoptotic cell death. Therefore, we measured mitochondrial membrane potential
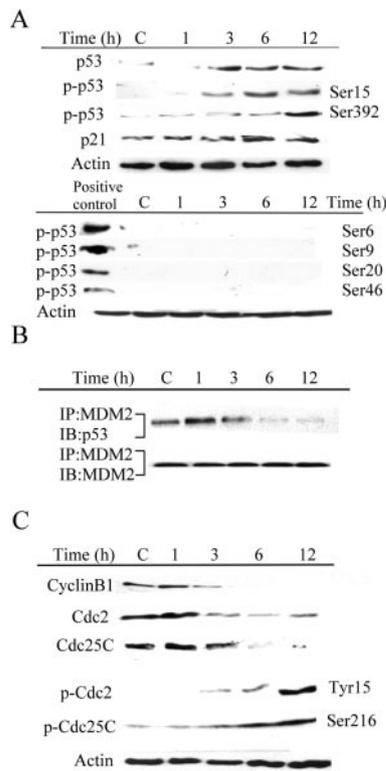
Fig. 3. The effect of plumbagin on cell cycle-related molecules. A, levels of p53, phospho-p53 and p21. B, association of p53 and MDM2 assay by immunoprecipitation assay. C, levels of cyclinB1, Cdc2, phospho-Cdc2, Cdc25C, and phospho-Cdc25C were assessed by immunoblot assay. Positive control, COS cell plus UV irradiation for phospho-p53 at Ser6, Ser9, and Ser20; MCF-7 cell plus UV irradiation for phospho-p53 at Ser46.

($\Delta\Psi$m) using the mitochondria-specific dye JC-1. We investigated mitochondrial dysfunction by measuring $\Delta\Psi$m in plumbagin-treated A549 cells at 8 and 12 h (Fig. 4B). Cytosolic extracts were prepared under conditions to preserve the mitochondria, and cytosolic cytochrome c protein levels were measured by immunoblotting analysis. Figure 4C shows that the cytosolic fraction from untreated A549 cells contained no detectable amounts of cytochrome c, whereas it did become detectable after 48 h of 20 μM plumbagin treatment in A549 cells (Fig. 4C).

Hallmarks of the apoptotic process include the activation of cysteine proteases, which represent both initiators and executors of cell death. Upstream caspase-9 activities increased significantly, as shown by the observation that treatment with plumbagin increased caspase-9 activity in A549 cells. This is consistent with the release of cytochrome c into the cytosol (Fig. 4D).

Plumbagin Induces the Activation of JNK. Figure 5A shows that activation (phosphorylation) of JNK was evident as early as 1 h after plumbagin treatment and persisted for the duration of the experiment. On the other hand, the expression of JNK (unphosphorylated form) was not altered by plumbagin treatment. Plumbagin-mediated activation of JNK was additionally confirmed by determining phosphorylation of one of its substrates, c-jun. As shown in Fig. 5B, in comparison with the control, the Ser63 phosphorylation of c-jun increased after A549 cells were exposed for 1 h to 20 μM plumbagin. Phosphorylation of c-jun increased relative to the control at all four time points (Fig. 5B).
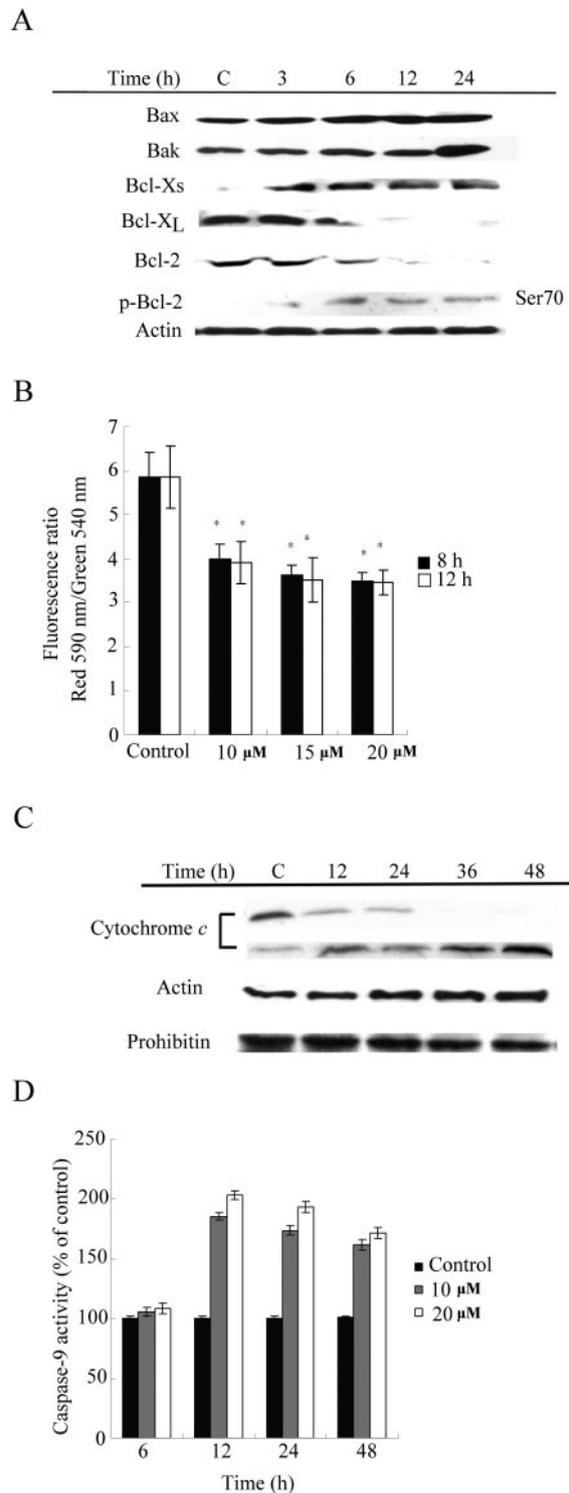

Fig. 4. Plumbagin induced apoptosis through the initiation of the mitochondrial pathway. A, expression level of Bcl-2 family proteins. B, loss of $\Delta\Psi$m. C, release of cytochrome c. D, activation of caspase-9. For A and C, cells were treated with 20 μM plumbagin for the indicated times. The cytoplasm and mitochondria were extracted from cell pellets by lysis buffer and centrifugation, and the levels of Bcl-2 and cytochrome c were assessed by immunoblot assay. For B, cells were treated with various concentrations of plumbagin for 8 and 12 h. The $\Delta\Psi$m was measured by JC-1 and flow cytometry. For D, cells were treated with 10 or 20 μM plumbagin for the indicated times, and the activity of caspase-9 was assessed by the caspase-9 activity assay kit. Each value is the mean $\pm$ S.D. of three determinations.
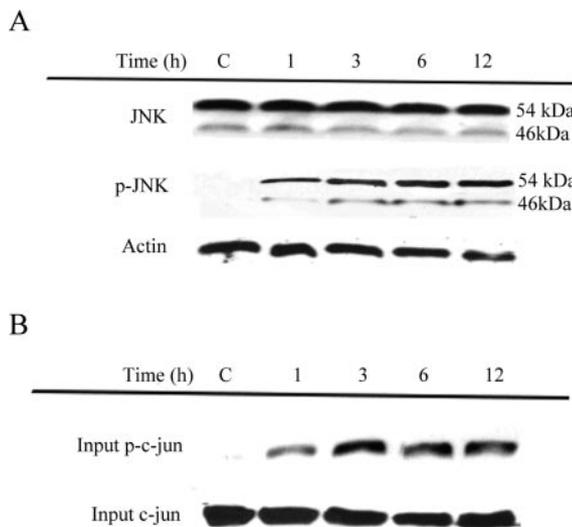
Fig. 5. Effect of plumbagin on expression and phosphorylation of JNK (A) as well as the activity of JNK. For A, the cells were treated with 20 μM plumbagin at different times. The control cells received an equal volume of DMSO. The cell lysates were prepared, and immunoblot assay was performed using antibodies against JNK and phospho-JNK. For B, the JNK kinase activity was determined using JNK Activity kit from Cell Signaling Technology according to the manufacturer's instructions.

The Role of p53 in Plumbagin-Mediated Cell Cycle Arrest and Apoptosis. To further define the role of p53 in plumbagin-induced cell cycle arrest and apoptosis, we transfected pCMV-p53mt135 plasmid containing the gene encoding a dominant-negative mutation of p53 that blocks normal p53 activity (Hsu et al., 2005). Overexpression of mutant p53 protein in cells transfected with the dominant-negative p53 mutant plasmid was verified by Western blot using antibody against human p53 (recognizing both wild- and mutant-type p53) (Fig. 6A). Cells expressing p53 mutant were subsequently used to document plumbagin-mediated cell cycle arrest and apoptosis. As shown in Fig. 6B, the inhibition of p53 activity was accompanied by a reduction in the sensitivity of A549 cells to plumbagin-mediated G$_2$/M arrest. The expression of p21 was also inhibited in pCMV-p53mt-transfected A549 cells (Fig. 6C). Furthermore, compared with vehicle-treated cells, induction of apoptosis induced by 20 μM plumbagin decreased from 36.5% in A549 cells to 13.4% in p53 mutant cells after a 24-h treatment (Fig. 6D). However, the inhibition of p53 did not completely abrogate plumbagin-mediated cell cycle arrest and apoptotic death, suggesting that plumbagin-mediated cell cycle arrest and apoptosis is carried through both p53-dependent and -independent manners.

Decrease of Plumbagin-Induced Cell Cycle Arrest and Apoptosis by JNK Chemical Inhibitors. To verify the possible role of JNK in plumbagin-induced apoptosis, A549 cells were pretreated for 1 h with the specific inhibitor for JNK, SP600125. Subsequently, the inhibitor-treated cells were exposed to plumbagin, and then cell cycle distribution and apoptosis were determined. As shown in Fig. 7A, the plumbagin-mediated JNK activation was effectively inhibited by 20 μM SP600125. Flow cytometric analysis of A549 cells exposed to plumbagin for 6 h showed that SP600125 partially blocked plumbagin-mediated G$_2$/M progression (Fig. 7B). Figure 7C shows the effect of JNK inhibitor almost completely abrogating plumbagin-induced apoptosis in A549

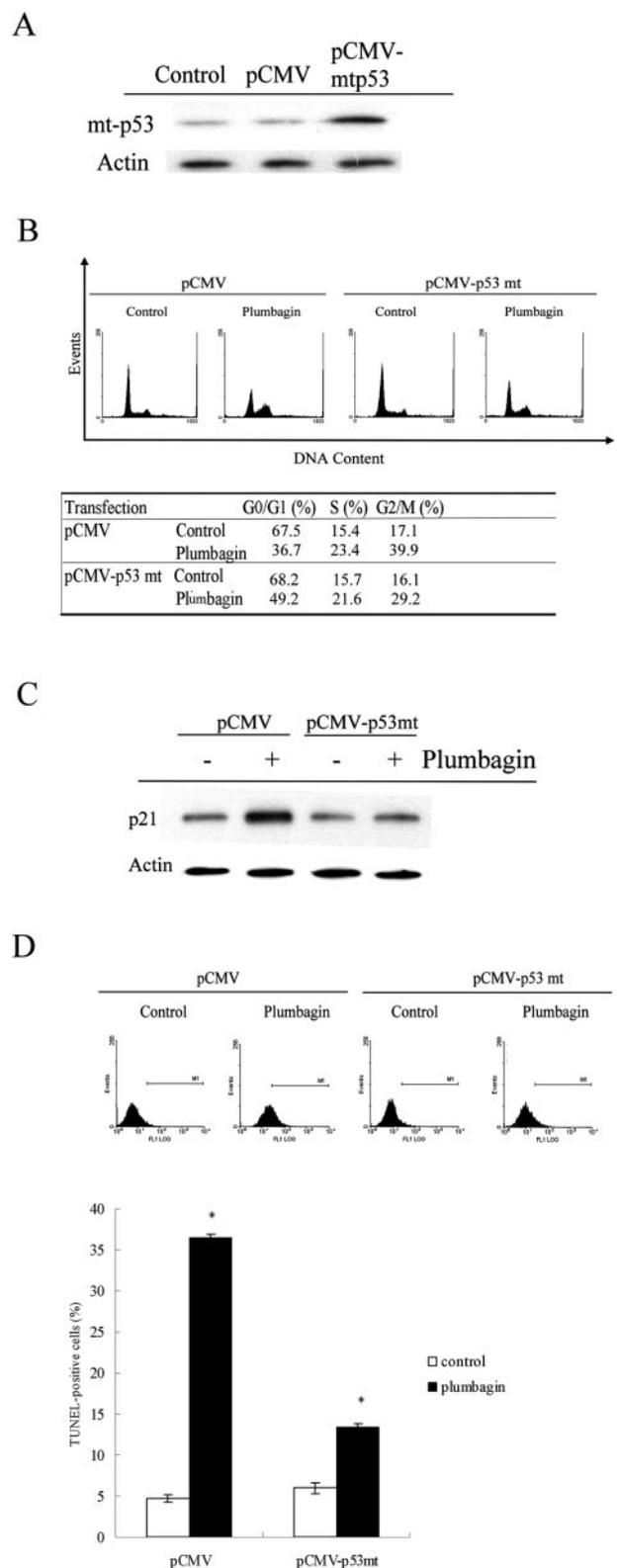| Transfection		G0/G1 (%)	S (%)	G2/M (%)
pCMV	Control	67.5	15.4	17.1
	Plumbagin	36.7	23.4	39.9
pCMV-p53 mt	Control	68.2	15.7	16.1
	Plumbagin	49.2	21.6	29.2

Fig. 6. Effect of p53 inhibition on plumbagin-mediated cell cycle arrest and apoptotic cell death. A, expression of p53mt in stable pCMV-p53mt-transfected A549 cells. B, p53 inhibition decreased the effect of plumbagin on cell cycle arrest, p21 levels (C), and apoptosis induction (D). A549 cells and mutant p53-transfected A549 cells were treated with 20 μM plumbagin for 6 (cell cycle assay) and 24 h (apoptosis assay). The induction of apoptosis was determined by PI stain and TUNEL analysis. Each value is the mean $\pm$ S.D. of three determinations. *, significant difference between control and plumbagin-treated cells, as analyzed by Dunnett's test ($p < 0.05$).
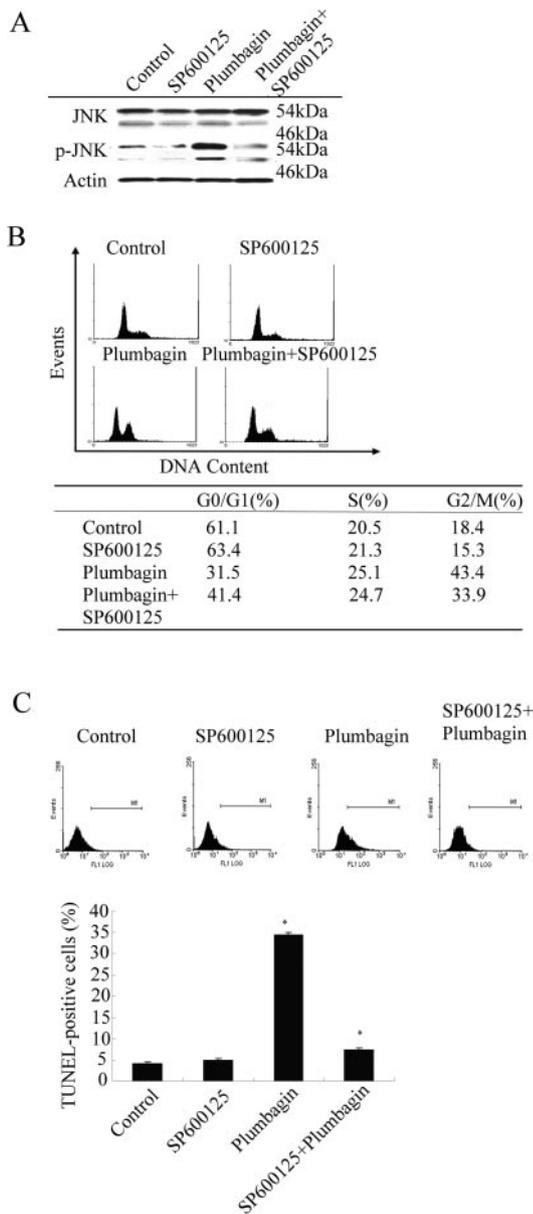
A

B

	G0/G1(%)	S(%)	G2/M(%)
Control	61.1	20.5	18.4
SP600125	63.4	21.3	15.3
Plumbagin	31.5	25.1	43.4
Plumbagin+ SP600125	41.4	24.7	33.9

C

Fig. 7. Effect of treatment of A549 cells with the JNK inhibitor SP600125 on plumbagin-mediated activation of JNK (A). The G_2/M arrest effect of plumbagin was inhibited by SP600125 (B). The induction of apoptosis was inhibited by SP600125 in plumbagin-treated cells (C). For all blocking experiments, cells were incubated for 1 h in the presence or absence of 20 μM SP600125, then 20 μM plumbagin was added and incubated for specific times (3 h for JNK activity, 24 h for apoptosis assay, and 6 h for cell cycle analysis). The activation of JNK was measured as described in the legend of Fig. 5. The induction of apoptosis was estimated by TUNEL analysis. Cell cycle distribution was assessed by flow cytometric analysis. Each value is the mean ± S.D. of three determinations.

cells. In comparison with control cells, the percentage of apoptotic cells was significantly higher in cultures exposed to 20 μM plumbagin, but this effect was blocked by the JNK inhibitor at 24 h (Fig. 7C).

The Role of JNK on p53 and Bcl-2 Phosphorylation. Previous studies have indicated that p53 phosphorylation at Ser15 is a critical event for stabilizing the function of p53. Phosphorylation at this site in vivo was shown to be inhibited by JNK-specific inhibitors, suggesting that JNK may target this serine directly or indirectly (Milne et al., 1995; Fuchs et al., 1998). As shown in Fig. 8A, pretreatment of cells with
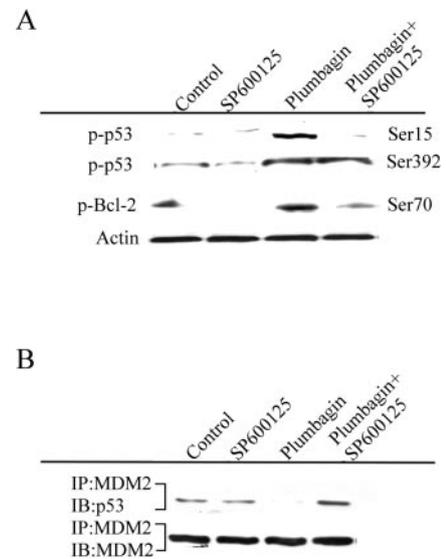
A

B

Fig. 8. SP600125 inhibits the effect of plumbagin on p53 and Bcl-2 phosphorylation. A, SP600125 inhibits the up-regulation of p53, phospho-p53 (Ser15), and phospho-Bcl-2 (Ser70). B, inhibition by plumbagin on p53-MDM2 interaction was decreased by SP600125. Cells were incubated for 1 h in the presence or absence of 20 μM SP600125, then 20 μM plumbagin was added and incubated for 6 (for p53) and 12 (for Bcl-2) h. The levels of p53 and Bcl-2 were assessed by immunoblot analysis.

SP600125 decreased the plumbagin induction of p53 protein and phosphorylation at Ser15. Moreover, a major factor that influences the stability of p53 protein is the binding of p53 with MDM2, and this interaction is inhibited when p53 phosphorylation occurred. As shown in Fig. 8B, the binding of MDM2 to p53 dramatically decreased in plumbagin-treated cells. These data suggest that plumbagin induces p53 phosphorylation through JNK signaling, which stabilizes p53 protein to induce p21 expression.

On the other hand, we tested the involvement of the mitochondrial apoptotic pathway by examining the effect of JNK inhibitors on phospho-Bcl-2 expression. As shown in Fig. 8A, cotreatment of A549 cells with plumbagin and SP600125 completely blocked plumbagin-mediated Bcl-2 phosphorylation at Ser70.

Plumbagin Inhibits Tumor Growth in Nude Mice. To determine whether plumbagin inhibits tumor growth in vivo, equal numbers of A549 cells were injected s.c. into both flanks of the nude mice. Tumor growth inhibition was most evident in mice treated with plumbagin at 2 mg/kg/day, where ~80% reductions in tumor size were observed, in contrast with mice treated with the vehicle (Fig. 9, A and B). No sign of toxicity, as judged by parallel monitoring body weight, was observed in plumbagin-treated mice.

To gain insight into the mechanism of plumbagin's inhibition of tumor growth in vivo, we harvested the A549 tumor xenografts from vehicle- and plumbagin-treated mice after treatments and assessed apoptosis by TUNEL analysis. We also extracted proteins to assess for levels of phospho-p53, phospho-JNK, cleaved PARP, and activated caspase-3 proteins. As shown in Fig. 9C, increase of TUNEL-positive cells were observed in tumors of the plumbagin-treated mice, compared with tumors of vehicle-treated mice. In addition, the PARP cleavage, caspase-3 activation, phospho-p53 (Ser15), and phospho-JNK levels increased in the tumors from the
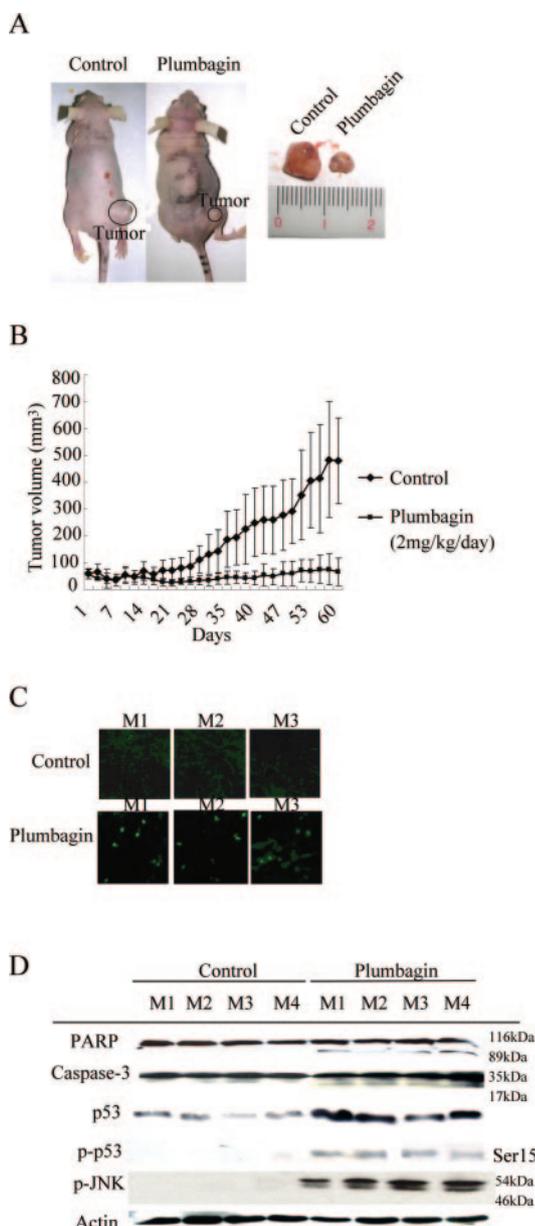
A

Control   Plumbagin

B

C

M1   M2   M3

Control

M1   M2   M3

Plumbagin

D

Fig. 9. Plumbagin inhibits growth and induces apoptosis of A549 xenograft by increasing p53 expression and activating JNK. A, representative tumor-possessing nude mice and tumors from the control and plumbagin-treated groups. B, mean of tumor volume measured at the indicated number of days after implant. C, plumbagin induces apoptosis in A549 xenograft by TUNEL assay. D, cleavage of PARP and caspase-3 and expression of p53 and JNK in A549 xenograft. Animals bearing pre-established tumors ($n = 15$ per group) were dosed daily for 60 days with i.p. injections of plumbagin (2 mg/kg/day) or vehicle. During the 60-day treatment, tumor volumes were estimated using measurements taken from external calipers (millimeters cubed). Apoptosis was assessed by TUNEL assay. The levels of PARP, caspase-3, p53, phospho-p53, and phospho-JNK were assessed by immunoblot analysis. Each value is the mean ± S.D. of three determinations. ∗, significant difference between control and plumbagin-treated cells, as analyzed by Dunnett's test ($p < 0.05$).

plumbagin-treated group compared with tumors from vehicle-treated mice (Fig. 9D).

Discussion

Lung cancer is the most common neoplasm in human in both developed and developing countries (Raez and Lilen-

baum, 2004). In our study, we have found that plumbagin effectively inhibits tumor cell growth in vitro, concomitant with induction of cell cycle arrest and apoptosis, and inhibits tumor cell growth in nude mice. Furthermore, because plumbagin does not exhibit any significant toxicity on normal lung cancer, this suggests that plumbagin possesses selectivity between normal and cancer cells.

Tumor suppressor gene p53 is a key element in the induction of cell cycle arrest and apoptosis following DNA damage or cellular stress in human cells (Harris and Levine, 2005). Cell cycle arrest that is dependent on p53 requires transactivation of p21 or other cell cycle-related factors (Taylor and Stark, 2001). The induction of p21 causes subsequent arrest in the G_1/G_0 or G_2/M phase of the cell cycle by binding of the cyclin-cdk complex (Taylor and Stark, 2001; Coqueret, 2003). In this study, we have shown that treatment of A549 cells with plumbagin resulted in the accumulation of p53 and phospho-p53 (Ser15 and 392) both in vivo and in vitro. Indeed, we also have found that plumbagin increases the expression of p21 and arrests the cell cycle at G_2/M. The upregulation of p21 by plumbagin was inhibited by suppression of normal p53 activity via dominant-negative p53, suggesting that p21 is regulated in a p53-dependent manner. In addition, treatment of A549 with plumbagin also decreases the expression of cyclinB1, Cdc25C, and Cdc2, whereas it increases the phosphorylation of Cdc2 and phospho-Cdc25C. Therefore, we suggest that plumbagin may prove to be a valuable tool for inhibition of Cdc2/cyclinB1 in lung cancers for the following reasons: the down-regulation of cyclinB1 by plumbagin; the induction of p21 by plumbagin in a p53-dependent manner, which may subsequently inhibit the function of Cdc2 by forming Cdc2/p21 complex; and the increase of phospho-Cdc25C followed by an increase in inactivated phospho-Cdc2, suggesting that increased phospho-Cdc25C levels may also decrease functioning phosphatase for dephosphorylating and activating Cdc2.

Increased expression of p21 is associated with cell cycle inhibition, differentiation, and cellular senescence (Chen at al., 2002). In addition, p21 can bind to proliferating cell nuclear antigen, thereby blocking DNA synthesis (Gartel and Radhakrishnan, 2005). Jaiswal et al. (2002) have indicated that plumbagin treatment caused an increase of p21 expression and a decrease of DNA repair resulting in cell death in mouse embryonic fibroblast cells. However, p21 has also been reported to influence the outcome of the p53 response to DNA damage and play a protective role on survival signal against apoptosis (Seoane et al., 2002; Kuo et al., 2004). The up-regulation of p21 by p53 induction attenuates the cell death in the quercetin-treated A549 cells (Kuo et al., 2004). These different observations may be due to the cell type and cell content specificity of apoptosis inducers and their subsequent signaling transduction pathways. Although our result indicated that plumbagin induces early G_2/M phase arrest, which is followed by apoptosis in A549 cells, the actual role of p21 in the relation of G_2/M arrest and apoptosis requires further investigation.

Mitochondrial apoptotic pathway has been described as an important signaling of apoptotic cell death for mammalian cells (Hengartner, 2000). Following the treatment of A549 cells with plumbagin, we observed that plumbagin treatment resulted in a significant increase of Bax and Bak, Bcl-Xs expression, and a decrease of Bcl-2 and Bcl-X_L, suggesting

that changes in the ratio of proapoptotic and antiapoptotic Bcl-2 family proteins might contribute to the apoptosis promotion activity of plumbagin. In addition, elevation of phospho-Bcl-2 (Ser70) by plumbagin treatment further helps reduce its ability to bind with Bax and enhance the translocation of Bax from cytosol to mitochondria, leading to an enhanced susceptibility of the cells to apoptosis (Ishikawa et al., 2003; Zu et al., 2005). However, phosphorylation of Bcl-2 at Ser70 has also been reported to be required for Bcl-2's antiapoptotic activity upon IL-3 and etoposide treatment (Ito et al., 1997; Deng et al., 2001). The influence of Bcl-2 phosphorylation thus requires further investigation. Our finding also showed a collapse of $\Delta\Psi m$, a substantial release of cytochrome c, and the activation of caspase-9 after A549 cells were treated with plumbagin. These occurrences of mitochondria apoptotic events are correlated with the modulation of plumbagin on Bcl-2 family proteins. These results confirm that plumbagin-induced apoptosis is associated with regulation of Bcl-2 family proteins.

Activation of the JNK pathways has long been associated with the apoptotic response induced by several DNA-damaging agents (Liu and Lin, 2005). The proapoptotic targets of the activated JNK are not clearly defined, but the phosphorylation of transcription factors such as c-Jun and p53, as well as pro- and antiapoptotic Bcl-2 family members such as Bim and Bcl-2, has been suggested to be of importance (Fuchs et al., 1998; Buschmann et al., 2000; Liu and Lin, 2005; Yoshida et al., 2005). Phosphorylation of human p53 in the N-terminal domain results in enhancement of transcriptional activity and prolongation of p53 half-life by inhibiting p53-MDM2 complex formation (Fuchs et al., 1998; Buschmann et al., 2000). In this report, we have shown that treatment of A549 cells with plumbagin resulted in the accumulation of phospho-JNK in both in vitro and in vivo. This JNK activation correlated well with the plumbagin-induced increase of JNK activity as measured by the JNK substrate phospho-c-Jun. Furthermore, we observed that blocking the plumbagin-induced activation of JNK1/2 by SP600125 could prevent p53 phosphorylation (Ser15) and enhance p53-MDM2 interaction, suggesting that plumbagin-induced JNK activation contributes to the stabilization of p53 function by Ser15 phosphorylation, which decreases the interaction of p53 and MDM2. This suggestion was strongly supported by the inhibition of the duration and phosphorylation of p53 (Ser15) by SP600125 treatment. Our results indicated that the Ser392 and Ser15 phosphorylation of p53 was also observed in plumbagin A549 cells, but SP600125 did not affect Ser392 phosphorylation on p53. Therefore, the upstream regulators and effect of p53 Ser392 phosphorylation require further investigation. Previous study has reported that Bcl-2 is inactivated by phosphorylation on three serine residues (Thr69, Ser70, and Ser87) via JNKs (Yamamoto et al., 1999). Our results showed that exposure of A549 cells to plumbagin led to concurrent phosphorylation of Bcl-2 at Ser70 and SP600125 pretreatment inhibited Bcl-2 phosphorylation, suggesting that the activation of JNK induced by plumbagin is involved in the modulation of Bcl-2. Moreover, the JNK inhibitor SP600125 prevented plumbagin-induced G_2/M arrest and apoptosis, further suggesting that the cooperation of JNK with p53 and the mitochondrial apoptotic pathway play a crucial role in plumbagin-induced G_2/M arrest and apoptosis.

Although SP600125 was described as an inhibitor of the

JNK pathway for the treatment of autoimmune, inflammatory, and neurodegenerative diseases and shown to be selective for JNK1/2 (Bennett et al., 2001), it has also been reported to exhibit nonspecific inhibition on several cell cycle and apoptosis-related enzymes, including serum- and glucocorticoid-induced kinase, p70 ribosomal protein S6 kinase, AMP-activated protein kinase, Cdk2, and dual-specificity, tyrosine-phosphorylated and regulated kinase 1A (Bain et al., 2003). Therefore, the influence of nonspecific inhibition of SP600125 on plumbagin-mediated cell cycle arrest and apoptosis induction could be further investigated.

In conclusion, the present study demonstrated that human nonsmall cell lung cancer A549 cells are highly sensitive to growth inhibition by plumbagin both in in vitro and in vivo experimental models; reduced survival of A549 cells after exposure to plumbagin is associated with G_2/M phase cell cycle arrest and apoptosis induction; plumbagin can inhibit cell cycle progression at the G_2/M phase by increasing p21 expression in a p53-dependent manner and by decreasing the expression of Cdc2, Cdc25C, and cyclinB1; plumbagin-induced cell growth inhibition in the A549 cells is mediated by activation of JNK, which stabilizes p53 by phosphorylation of p53 at Ser15 and decreasing the interaction of p53 and MDM2; and JNK also phosphorylates Bcl-2, leading to alter function of Bcl-2 to apoptosis. These findings suggest that plumbagin may be a promising chemopreventive agent against human nonsmall cell lung cancer.

References

Bain J, McLauchlan H, Elliott M, and Cohen P (2003) The specificities of protein kinase inhibitors: an update. *Biochem J* **371:**199–204.
Bennett BL, Sasaki DT, Murray BW, O'Leary EC, Sakata ST, Xu W, Leisten JC, Motiwala A, Pierce S, Satoh Y, et al. (2001) SP600125, an anthrapyrazolone inhibitor of Jun N-terminal kinase. *Proc Natl Acad Sci USA* **98:**13681–13686.
Bode AM and Dong Z (2004) Post-translational modification of p53 in tumorigenesis. *Nat Rev Cancer* **4:**793–805.
Buschmann T, Adler V, Matusevich E, Fuchs SY, and Ronai Z (2000) p53 phosphorylation and association with murine double minute 2, c-Jun NH$_2$-terminal kinase, p14ARF and p300/CBP during the cell cycle and after exposure to ultraviolet irradiation. *Cancer Res* **60:**896–900.
Chen C, Shen G, Hebbar V, Hu R, Owuor ED, and Kong AN (2003) Epigallocatechin-3-gallate-induced stress signals in HT-29 human colon adenocarcinoma cells. *Carcinogenesis* **24:**1369–1378.
Chen X, Zhang W, Gao YF, Su XQ, and Zhai ZH (2002) Senescence-like changes induced by expression of p21(waf1/Cip1) in NIH3T3 cell line. *Cell Res* **12:**229–233.
Coqueret O (2003) New roles for p21 and p27 cell-cycle inhibitors: a function for each cell compartment? *Trends Cell Biol* **13:**65–70.
Deng X, Xiao L, Lang W, Gao F, Ruvolo P, and May WS Jr (2001) Novel role for JNK as a stress-activated Bcl2 kinase. *J Biol Chem* **276:**23681–23688.
Ding Y, Chen ZJ, Liu S, Che D, Vetter M, and Chang CH (2005) Inhibition of Nox-4 activity by plumbagin, a plant-derived bioactive naphthoquinone. *J Pharm Pharmacol* **57:**111–116.
Freedman VH and Shin SI (1974) Cellular tumorigenicity in nude mice: correlation with cell growth in semi-solid medium. *Cell* **3:**355–359.
Fuchs SY, Adler V, Pincus MR, and Ronai Z (1998) MEKK1/JNK signaling stabilizes and activates p53. *Proc Natl Acad Sci USA* **95:**10541–10546.
Gao Y, Signore AP, Yin W, Cao G, Yin XM, Sun F, Luo Y, Graham SH, and Chen J (2005) Neuroprotection against focal ischemic brain injury by inhibition of c-Jun N-terminal kinase and attenuation of the mitochondrial apoptosis-signaling pathway. *J Cereb Blood Flow Metab* **25:**694–712.
Gartel AL and Radhakrishnan SK (2005) Lost in transcription: p21 repression, mechanisms and consequences. *Cancer Res* **65:**3980–3985.
Harris SL and Levine AJ (2005) The p53 pathway: positive and negative feedback loops. *Oncogene* **24:**2899–2908.
Hengartner MO (2000) The biochemistry of apoptosis. *Nature (Lond)* **407:**770–776.
Hsieh YJ, Lin LC, and Tsai TH (2005) Determination and identification of plumbagin from the roots of *Plumbago zeylanica* L. by liquid chromatography with tandem mass spectrometry. *J Chromatogr A* **1083:**141–145.
Hsu YL, Kuo PL, and Lin CC (2005) Isoliquiritigenin induces apoptosis and cell cycle arrest through p53-dependent pathway in HepG2 cells. *Life Sci* **77:**279–292.
Ito T, Deng X, Carr B, and May WS (1997) Bcl-2 phosphorylation required for anti-apoptosis function. *J Biol Chem* **272:**11671–11673.
Ishikawa Y, Kusaka E, Enokido Y, Ikeuchi T, and Hatanaka H (2003) Regulation of Bax translocation through phosphorylation at Ser-70 of Bcl-2 by MAP kinase in NO-induced neuronal apoptosis. *Mol Cell Neurosci* **24:**451–459.
Jaiswal AS, Bloom LB, and Narayan S (2002) Long-patch base excision repair of apurinic/apyrimidinic site DNA is decreased in mouse embryonic fibroblast cell

lines treated with plumbagin: involvement of cyclin-dependent kinase inhibitor p21Waf-1/Cip-1. *Oncogene* **21:**5912–5922.

Kelly K (2005). The role of targeted agents in adjuvant therapy for non-small cell lung cancer. *Clin Cancer Res* **11:**5027s–5029s.

Kuo PC, Liu HF, and Chao JI (2004) Survivin and p53 modulate quercetin-induced cell growth inhibition and apoptosis in human lung carcinoma cells. *J Biol Chem* **279:**55875–55885.

Liu J and Lin (2005) Role of JNK activation in apoptosis: a double-edged sword. *Cell Res* **15:**36–42.

Martin EJ and Forkert PG (2004) Evidence that 1,1-dichloroethylene induces apoptotic cell death in murine liver. *J Pharmacol Exp Ther* **310:**33–42.

Milne DM, Campbell LE, Campbell DG, and Meek DW (1995) p53 is phosphorylated in vitro and in vivo by an ultraviolet radiation-induced protein kinase characteristic of the c-Jun kinase, JNK1. *J Biol Chem* **270:**5511–5518.

Mossa JS, El-Feraly FS, and Muhammad I (2004) Antimycobacterial constituents from *Juniperus procera*, *Ferula communis* and *Plumbago zeylanica* and their in vitro synergistic activity with isonicotinic acid hydrazide. *Phytother Res* **18:**934–937.

Raez LE and Lilenbaum R (2004) Chemotherapy for advanced non-small-cell lung cancer. *Clin Adv Hematol Oncol* **2:**173–178.

Robles AI, Linke SP, and Harris CC (2002) The p53 network in lung carcinogenesis. *Oncogene* **21:**6898–6907.

Seoane J, Le HV, and Massague J (2002) Myc suppression of the p21(Cip1) Cdk inhibitor influences the outcome of the p53 response to DNA damage. *Nature (Lond)* **419:**729–734.

Shin SI, Freedman VH, Risser R, and Pollack R (1975) Tumorigenicity of virus-transformed cells in nude mice is correlated specifically with anchorage independent growth in vitro. *Proc Natl Acad Sci USA* **72:**4435–4439.

Singh UV and Udupa N (1997) Reduced toxicity and enhanced antitumor efficacy of betacyclodextrin plumbagin inclusion complex in mice bearing Ehrlich ascites carcinoma. *Indian J Physiol Pharmacol* **41:**171–175.

Srinivas P, Gopinath G, Banerji A, Dinakar A, and Srinivas G (2004) Plumbagin induces reactive oxygen species, which mediate apoptosis in human cervical cancer cells. *Mol Carcinog* **40:**201–211.

Sugie S, Okamoto K, Rahman KM, Tanaka T, Kawai K, Yamahara J, and Mori H (1998) Inhibitory effects of plumbagin and juglone on azoxymethane-induced intestinal carcinogenesis in rats. *Cancer Lett* **127:**177–183.

Taylor WR and Stark GR (2001) Regulation of the G_2/M transition by p53. *Oncogene* **20:**1803–1815.

Xu D, Falke D, and Juliano RL (2003) p53-dependent cell-killing by selective repression of thymidine kinase and reduced prodrug activation. *Mol Pharmacol* **64:**289–2897.

Xu YC (2003) Regulation of p53 responses by post-translational modifications. *Cell Death Differ* **10:**400–403.

Yamamoto K, Ichijo H, and Korsmeyer SJ (1999) BCL-2 is phosphorylated and inactivated by an ASK1/Jun N-terminal protein kinase pathway normally activated at G_2/M. *Mol Cell Biol* **19:**8469–8478.

Yoshida K, Yamaguchi T, Natsume T, Kufe D, and Miki Y (2005) JNK phosphorylation of 14-3-3 proteins regulates nuclear targeting of c-Abl in the apoptotic response to DNA damage. *Nat Cell Biol* **7:**278–285.

Zu K, Hawthorn L, and Ip C (2005) Up-regulation of c-Jun-NH2-kinase pathway contributes to the induction of mitochondria-mediated apoptosis by alpha-tocopheryl succinate in human prostate cancer cells. *Mol Cancer Ther* **4:**43–50.

Address correspondence to: Dr. Chun-Ching Lin, Graduate Institute of Natural Products, College of Pharmacy, Kaohsiung Medical University, 100 Shih-Chuan 1st Road, Kaohsiung 807, Taiwan. E-mail: aalin@ms24.hinet.net